ADVANCED ELECTRONIC MATERIALS
www.advelectronicmat.de

All-Solid-State Organic Schmitt Trigger Implemented by Twin Two-in-One Ferroelectric Memory Transistors

*Sunbin Hwang, Sukjae Jang, Sukang Bae, Seoung-Ki Lee, Sang Hyun Lee, Simone Fabiano, Magnus Berggren, Takhee Lee, and Tae-Wook Kim**

Although there have been many attempts to replace conventional inorganic electronics with organic materials that can be mass produced at low cost, few organic electronic filters to increase immunity to electrical noise have been reported thus far. Conventional Schmitt triggers or their inverters are used in many electronic circuits as versatile electronic noise filters. However, it is challenging to manufacture organic electronic systems with complex circuitry. In this study, a simple, all-solid-state organic Schmitt trigger consisting of twin two-in-one organic ferroelectric memory transistors with the same chemical compositions and device dimensions but different threshold voltages is introduced. Threshold voltages and hysteresis in the two-in-one devices can be controlled by polarization switching as demonstrated in a previous study. Hysteresis of a ferroelectric p-type depletion load inverter can be achieved using twin two-in-one devices when the sweep voltage is higher than the critical gate voltages. This facilitates inverter characteristics at two different threshold voltages, and realizing a Schmitt trigger. Finally, based on simulation program with integrated circuit emphasis (SPICE) simulation, guidelines are proposed on how to design organic Schmitt triggers with p- or n-type materials and ferroelectric or charge-trapping mechanisms to achieve inverting or non-inverting characteristics.

1. Introduction

Electrical properties of various organic materials can be modulated by tailoring functional groups, resulting in organic electronics with versatile functionalities.[1–4] Organic compounds also have the advantages of being lightweight and flexible in addition to being amenable to low-temperature solution processing, which could enable roll-to-roll mass printing of large-area electronics and integrated modules at reduced cost.[5–14] Organic light-emitting diodes (LEDs)are famous commercialized organic devices used as display modules in smartphones. However, other electronic components have not been completely replaced by organic materials yet because of the poor performance and lifetime of these materials. Several research groups have therefore focused their efforts on developing various electronic elements from organic materials such as electrodes, capacitors, inductors, memory, photovoltaic cells, sensors, transistors, and non-volatile memory for complex electronic devices.[15–17] Nevertheless, only a few organic electronic filters for circuits with noisy electric signals have been reported.

A Schmitt trigger, one of the most commonly used versatile noise filters, consists of a comparator circuit with hysteresis that is induced by applying positive feedback to the non-inverting input of a comparator or differential amplifier. These characteristics of a Schmitt trigger allow the output signal to retain its signal until the input signal changes enough to change the trigger, hence use of the term "trigger."[18] One of representative use of a Schmitt trigger is as an electric noise filter in integrated circuits. It is particularly effective in signaling conditioning applications such as increasing immunity to noise in circuits caused by contact bounce in switches or fluctuations from unpredictable output changes. Another use of a Schmitt trigger is an one-bit analog-to-digital converter, which transform an analog input to a digital output signals using a low-to-high signal transition

Prof. T.-W. Kim
Department of Flexible and Printable Electronics
Jeonbuk National University
567 Baekje-daero, Deokjin-gu, Jeonju 54896, Republic of Korea
E-mail: twk@jbnu.ac.kr

Prof. T. Lee
Department of Physics and Astronomy
Institute of Applied Physics
Seoul National University
Seoul 08826, Republic of Korea

The ORCID identification number(s) for the author(s) of this article can be found under https://doi.org/10.1002/aelm.201901263.

DOI: 10.1002/aelm.201901263

Prof. S. Fabiano, Prof. M. Berggren
Laboratory of Organic Electronics
Department of Science and Technology
Linköping University
Norrköping SE-601 74, Sweden

Prof. S. H. Lee
School of Chemical Engineering
Chonnam National University
77 Yongbong-ro
Buk-gu, Gwangju 61186, Republic of Korea

Dr. S. Hwang, Dr. S. Jang, Dr. S. Bae, Dr. S.-K. Lee
Functional Composite Materials Research Center
Korea Institute of Science and Technology
Wanju, Jeollabuk-do 55324, Republic of Korea

ADVANCED ELECTRONIC MATERIALS
www.advelectronicmat.de

as the signal reaches a predetermined level.[19] Schmitt triggers can be used in relaxation oscillators, function generators, switching power supplies, and as basic elements of neuromorphic electronic systems.[20,21] Despite these diverse applications in electronic circuits, a typical Schmitt trigger requires complex circuitry and various electronic components (two transistors and six resistors in general). Therefore, it is still difficult to implement organic Schmitt triggers due to the poor processability of organic materials for active or passive components of the electronic circuit. Schmitt trigger usually has two emitter-coupled transistor stages or a non-inverting comparator (operational amplifier). For example, a bipolar junction transistor bistable collector-base coupled circuit can be a Schmitt trigger by connecting additional base resistors to one of the bases.[18,19]

In this study, we propose a simple, all-solid-state organic Schmitt trigger consisting of only two device components (twin devices) with the same chemical compositions and dimensions. To realize this all-solid-state organic Schmitt trigger, we developed a two-in-one organic ferroelectric memory transistor. The two-in-one organic ferroelectric memory transistor has an electrical switching function with negligible hysteresis in addition to a non-volatile data storage function under certain gate bias conditions. By controlling the ferroelectric properties of poly(vinylidene fluoride-trifluoroethylene) (P(VDF-TrFE)) through the photo-crosslinking with bis-perfluorobenzoazide (bis-FB-N_3), we achieved both high permittivity and ferroelectricity of the crosslinked polymer for electrical switching and data storage, respectively. These electrical characteristics enabled us to generate a ferroelectric p-type depletion load inverter composed of two transistors with the same chemical compositions and device configurations, but with different threshold voltages. The control of threshold voltages can simply be changed by polarization switching by using the characteristic of ferroelectric transistor.[22] We demonstrated an organic Schmitt trigger in which the threshold voltage and hysteresis of the ferroelectric p-type depletion load inverter can be freely controlled without any chemical treatment or change in device configuration. The hysteresis of the p-type depletion load inverter can be suppressed when sweep voltages are lower than the critical gate voltage, and it can be used as a general inverter with a single threshold voltage. Hysteresis is induced when the sweep voltages are larger than the critical gate voltage, yielding inverter characteristics with two threshold voltages. These electrical characteristics of the p-type depletion load inverter allow it to function as a Schmitt trigger, simplify the device configuration, and reduce power consumption. Based on our experimental results, we propose guidelines for how to design new inverting or non-inverting Schmitt triggers using only twin memory transistors with different types of channel materials or operational mechanisms through Simulation Program with Integrated Circuit Emphasis (SPICE) simulations.

2. Results and Discussion

2.1. Strategy to Make All-Solid-State Organic Schmitt Triggers Using Twin Two-in-One Ferroelectric Memory Transistors

Below we describe the strategy to make all-solid-state organic Schmitt triggers using twin two-in-one ferroelectric memory transistors in detail. A general transistor usually has one function that is the switching and amplifying of the current by gate bias. An organic ferroelectric transistor consists of π-conjugated organic molecules as an active channel and organic ferroelectric materials as a dielectrics layer, respectively.[23–25] As writing/deleting voltage biases are applied to the gate electrode of ferroelectric transistor, the drain current exhibits threshold voltage shifts, that is, hysteresis window, and indicates the typical non-volatile memory operation.[9,23–27] P(VDF-TrFE) is an insulating organic polymer that has great ferroelectric properties including a high remnant polarization and enough dielectric constant compared with those of other insulating polymers.[23,28] Because of above characteristic, P(VDF-TrFE) is generally used to ferroelectric memory transistors as a ferroelectric dielectric layer.

Our two-in-one organic ferroelectric memory transistor has an electrical switching with small hysteresis in additional to a non-volatile data storage functions. Motion of P(VDF-TrFE) was effectively restricted by photo-crosslinking via bis-FB-N_3, which conferred high permittivity and ferroelectricity for electrical switching function and data storage function, respectively. In addition, the threshold voltage of the two-in-one device was adjustable by modulating the amount of crosslinks in P(VDF-TrFE). Therefore, hysteresis-free electrical on/off switching of the device under relatively weak gate bias at the critical gate voltage was realized.

Ferroelectric properties of a p-type depletion load inverter consist of twin two-in-one devices made of photo-crosslinked P(VDF-TrFE) could be precisely controlled as shown in **Figure 1**. To demonstrate a p-type depletion load inverter configured by twin two-in-one devices, we prepared the top source–drain contact and a bottom gate device that can function as a non-volatile memory and field effect transistor. Photo-crosslinked P(VDF-TrFE) and pentacene were used as dielectric and channel layers, respectively. Top Au on the pentacene channel, length (L) of 50 µm and width (W) of 1000 µm, and Si substrate

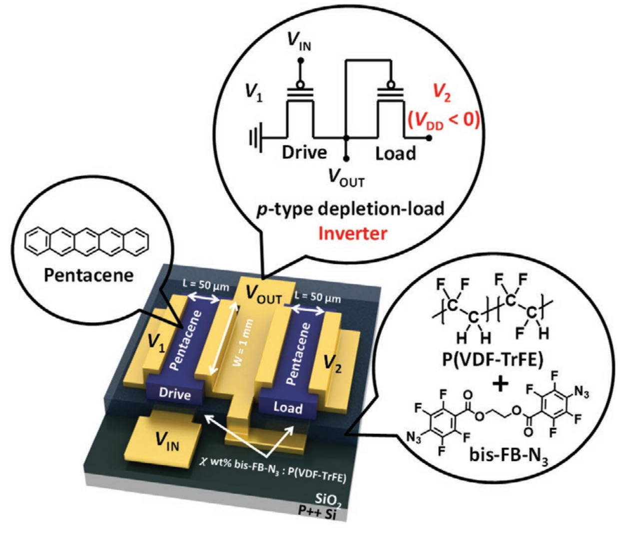

Figure 1. Schematic of a p-type depletion load inverter prepared by connecting twin two-in-one organic ferroelectric memory transistors of the same dimensions. The insets show an equivalent circuit of the device and the materials in the channel and dielectric layer.

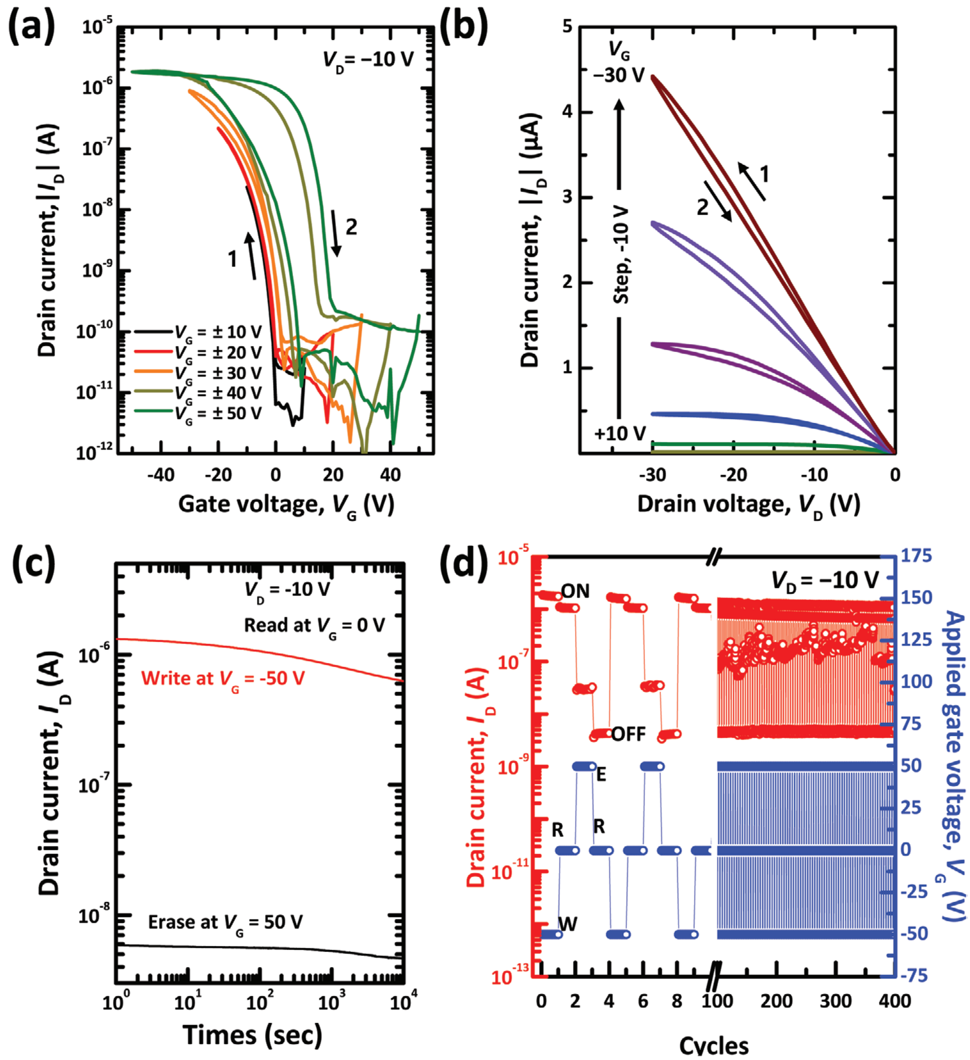

Figure 2. Electrical characteristics of the drive component in a p-type depletion load inverter consisting of twin two-in-one organic ferroelectric memory transistor. A pentacene and 17.6 wt% bis-FB-N_3:P(VDF-TrFE) are used as the channel and dielectric layers, respectively. a) Transfer and b) output characteristics. c) Retention time test for the written and erased states. d) Repeated write/read/erase/read (W-R-E-R) endurance cycling test for the series of gate voltages (V_G) of −50, 0, 50, and 0 V at a drain voltage (V_D) of −10 V. Sweep of V_G in transfer curves ranged from ±10 to ±50 V while V_D was maintained at −10 V. Sweep of V_D in output curves was varied from 0 to −30 V and V_G was swept from 10 to −30 V using −5 V steps.

were used for source–drain and gate electrode contacts, respectively. Further details are provided in Section 4. A dielectric layer with photo-crosslinked P(VDF-TrFE) (17.6 wt% bis-FB-N_3:P(VDF-TrFE)) was fabricated for the representative p-type depletion load inverter.

Figure 2 shows the electrical characteristics of the driver component in the p-type depletion load inverter. As shown in the drain current (I_D)–gate voltage (V_G) curves summarized in Figure 2a, the device showed typical transfer curves of p-type transistor with negligible hysteresis in the double gate voltage sweep range below ±30 V. The electrical noise is due to the gate leakage current as shown in Figure S3, Supporting Informartion. The gate leakage currents of 1 nA or less are almost same level as the noise in the low current region in all the voltage sweeps of the transfer curves. Nevertheless, we are sure that there are no problems on the performance and the reproducibility of the electrical characteristics of the devices, since only the characteristics in the high current range affect the actual device (Schmitt trigger).[23] In addition, output curves with negligible hysteresis were obtained by double sweeping the drain voltage from 0 to −30 V and the gate voltage from 10 to −30 V in steps of −5 V, as shown in Figure 2b. By contrast, double gate voltage sweep (±30 V higher than V_G) led to switching the polarization of the photocrosslinked P(VDF-TrFE) dielectric matrix, then clear hysteresis (i.e., memory window) was observed up to 13 V in the case of a ±50 V sweep. The retention time and write/read/erase/read (W-R-E-R) cycling tests are measured as memory operation parameters and shown in Figure 2c,d, respectively.

To determine the retention characteristics of the transistors, writing and erasing of the device were carried out by applying a V_G of −50 and +50 V, respectively. To read I_D after the writing and erase processes, drain voltage (V_D) and V_G were applied to −10 and 0 V each with a 1 s interval. The current level kept for more than 10^4 s as shown in Figure 2c. This indicates that retention time was at least 10^4 s or even more, and that the ON state can be maintained for that time after the writing process. The difference in measured I_D between the written and erased states remained constant at over 100 times during the retention test, indicating that the organic ferroelectric transistor had non-volatile memory characteristics. W-R-E-R cycling test also performed in order to verify the reversible switching properties and device reliability as shown in Figure 2d. The device exhibited durable reversible electrical switching under consecutive gate bias cycles without serious performance degradation during 400 cycles. Likewise, in the retention tests, an ON/OFF current ratio of two orders of magnitude was observed in the W-R-E-R cycling test. Consequently, the driver transistor in the p-type depletion load inverter clearly showed both data storage and electrical switching functions that can be obtained from a non-volatile memory transistor and typical transistors, respectively, as we reported previously for our two-in-one device.

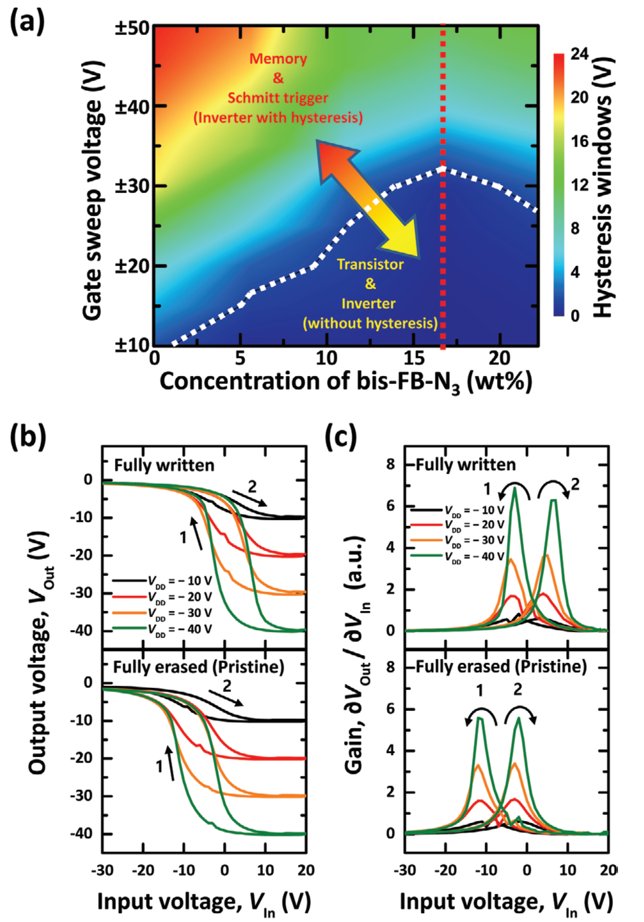

Figure 3. a) Contour plots of hysteresis windows as a function of bis-FB-N_3 content and V_G. The area below the white dashed line indicates a negligible hysteresis window that can be used as a general inverter, while the area above the white dashed line shows a sufficient hysteresis window for a Schmitt trigger. The red dashed line is representative of the p-type depletion load inverter in this paper that was implemented by twin two-in-one devices with pentacene as the channel layer and 17.6 wt% bis-FB-N_3:P(VDF-TrFE) as the dielectric layer. b) Output voltage (V_{Out}) transfer properties and c) the gain values of the p-type depletion load inverter, respectively, at fully written and erased (pristine) states of drive component under various power supply voltages (V_{DD} ranging from −10 to −40 V, with −10 V steps).

2.2. Electrical Characteristics of Schmitt Trigger Using a p-Type Depletion Load Inverter Consisting of Twin Two-in-One Ferroelectric Transistors

Next, based on the two-in-one ferroelectric memory transistor described above, we integrated a Schmitt trigger using a p-type depletion load inverter consisting of twin ferroelectric transistors. In general, an integrated circuit system has different electrical functions according to the specific connections or positions of the transistors in the circuit. Carrier type, drain current, and threshold voltages, can be modified to obtain the desired functions in a circuit system. For example, a depletion load inverter is usually used to implement logical negation and is configured by series connection of different operational mode transistors (enhancement and depletion modes). However, a two-in-one ferroelectric memory transistor can satisfy these conditions if each threshold voltages can be controlled simply. The change of threshold voltages can be performed by switching of polarization as described in Section 2.1. Thus, p-type depletion load inverters can be realized by connecting the twin transistors in series and by utilizing simple threshold voltage control affording by polarization switching of photocrosslinked P(VDF-TrFE) without changing W/L ratio and without the chemical modifications. Details of how to configure a depletion load inverter using twin transistors are provided below. As shown in Figure 1, the source electrode of the driver is coupled to both the drain and gate electrodes of the load in a p-type depletion load inverter. Subsequently, polarization switching is performed to balance the threshold voltages between driver and load components and make an inverter. To modulate the threshold voltages of each transistor, a V_G of +30 and −30 V was applied to write and erase, respectively, for 1 min at the fixed V_D of −10 V. In addition, input voltage (V_{In}) was dual swept from +20 to −30 V to induce hysteresis of the inverter because two different gain peaks, that is, an inverter with hysteresis, are necessary to achieve the Schmitt trigger.

The ferroelectricity of the P(VDF-TrFE) with regard to memory window changes as a function of bis-FB-N_3 content and applied gate voltage sweep ranges is described in more detail in our previous report.[22] Results are summarized in the contour plot in **Figure 3**a. The area below the white dashed line shows a negligible hysteresis window that can be used as a general inverter while, the area above the white dashed line shows a sufficient hysteresis window for a Schmitt trigger. Here, the white dashed line indicates the critical input sweep voltage above which the inverter shows hysteresis.

The red dashed line indicates a representative p-type depletion load inverter comprising a dielectric layer with photocrosslinked 17.6 wt% bis-FB-N_3:P(VDF-TrFE). Figure 3b,c shows the output voltage (V_{Out}) transfer characteristics for V_{In} sweeping from +20 to −30 V and the gain values of the inverter at fully written and erased (pristine) states of the driver under various power supply voltage (V_{DD}) conditions (from −10 to −40 V, with −10 V steps). The difference in critical voltage between a single memory transistor and an inverter incorporating twin two-in-one devices, that is, the sweep range of gate voltages where hysteresis begins to appear, is probably due to the sweep speed. General inverter operation with negligible hysteresis can also be obtained in the small V_{In} sweep range of 0 to −12 V but ferroelectric characteristics of photocrosslinked P(VDF-TrFE) cannot be induced in this sweep range.[22]

The difference in threshold voltage between drive and load results in a difference of current level, which enables inverter drive. A larger gate sweep voltage than the critical voltage causes hysteresis of outputs. The inverter gain, defined as $\partial V_{Out}/\partial V_{In}$, was estimated and a maximum gain (>5.0) for forward and reverse scans was achieved at V_{DD} = −40 V. The prepared inverter can be well converted to a logic output of "1" when the input signal is "0" and to the output signal of "0" when the input signal is "1" by means of V_{Out} at the boundary of each gain peak. Furthermore, the position of gain peaks can be freely adjusted by using the nonvolatile characteristics of the two-in-one device, as described later.

We next implemented a Schmitt trigger using a p-type ferroelectric depletion load inverter with two different gain peaks (see **Figure 4**). Various input signals (square, triangle, sine, and sine with random noise) as shown in Figure 4a were used to verify functioning of the Schmitt trigger as an electronic signal filter. In a Schmitt trigger with an inverting configuration (inverting Schmitt trigger) as shown in Figure 4b, outputs convert to low and high when the input signal is above the high threshold voltage and below the low threshold voltage, respectively. In contrast, when input signals are between the two levels, the output signal remains constant due to the dual threshold action of the Schmitt trigger. Additionally, these inverted output signals can be further inverted back to non-inverted signals by changing the configuration of the electrode connections. Further descriptions are provided in Section S1, Supporting Information.

Figure 4c shows the V_{Out} behavior of a fully written inverting Schmitt trigger for various input signals. For the device with a V_{DD} of −40 V and an inverting Schmitt trigger electrode configuration, V_{In}s of +30 and −30 V indicate inputs of 0 and 1, respectively. Thus, output both 1 and 0 were obtained at V_{Out} of −40 and 0 V, respectively. In the range of V_{In}s of +30 and–30 V, the transition threshold voltages of the inverter, which are the positions of the gain peaks as shown in Figure 3b, were +6.3 and −6.9 V, respectively, at the fully written state. Thus, various input signals were filtered through the Schmitt trigger and output signals with almost identical step shaped pulses were obtained. The slight phase deviation and small bend path noise seen in outputs in the ON state were due to the sine input and sine input with random noise, respectively. This band path noise and phase deviation may be caused by mismatch between the output range and the required input range for a clean switching operation.

The inverting Schmitt trigger provided an inverted output where the phase of the input signals was shifted by a half period, while the non-inverting Schmitt trigger provided a non-inverted output identical to the phase of the input signal. These signal conversions can be used for noise filtering, 1 bit analog-to-digital conversion, relaxation oscillators, function generators, switching power supplies, and as basic elements

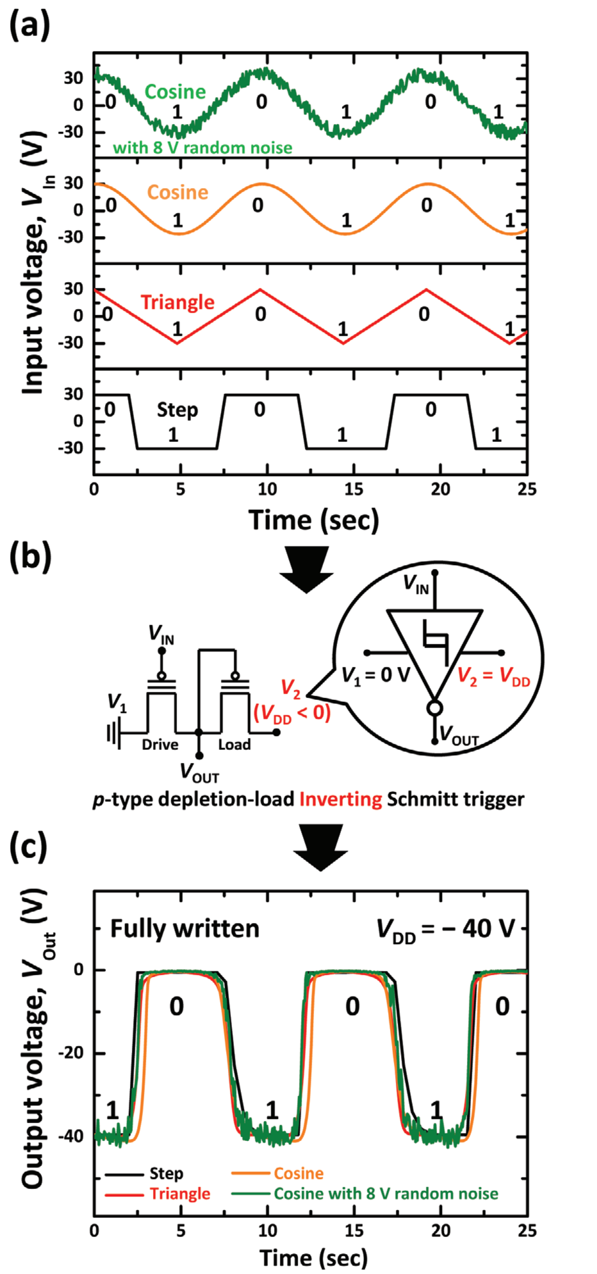

Figure 4. Output behavior of the fully written inverting and non-inverting Schmitt triggers for various input signals. a) Various input signals (squares, triangles, sines, and sines with 8 V random noise. b) Circuit diagrams and symbols of the inverting Schmitt trigger implemented by the p-type depletion load inverter. c) Output behavior of the inverting Schmitt trigger in response to various input signals.

of neuromorphic electronic systems as described earlier. In particular, the noise filtering applications of a Schmitt trigger can be used to clearly distinguish between ON/OFF states. For example, the ON/OFF state of a LED can be defined more stably and clearly by applying a Schmitt trigger. A single threshold switch cannot define a stable ON–OFF state due to rapid blinking at the boundary of a single threshold.

Because the operational voltage of the device is still high, it requires additional way to reduce power consumption of the devices. Minimizing the thickness of the dielectric layer may be a simple strategy to reduce the operational voltage of the device.[29,30] However, it is difficult to get a thin and smooth film by spincasting process, due to high boiling point solvent that deserved P(VDF-TrFE) in this work. Great care must be taken to resolve pin-holes and voids issues when fabricating an ultra-thin P(VDF-TrFE) film for lower operational voltage of the device. The thickness range of photocrosslinked P(VDF-TrFE) dielectric thin films were designed to be 235–317 nm in order to secure the high reproducibility of devices with dead-layer free even if the devices have high operational voltages in this study. Nevertheless, operational voltage of organic ferroelectric transistor is affected by complex reasons such as thickness of dielectric layer, quality of the film, and formation of dead-layer between the electrodes.

2.3. Pulse Width Modulation (PWM) Application Using a Schmitt Trigger in Response to Gain Peak Position Modulation

We next investigated the behavior of the inverting Schmitt trigger in response to gain peak position modulation of the p-type

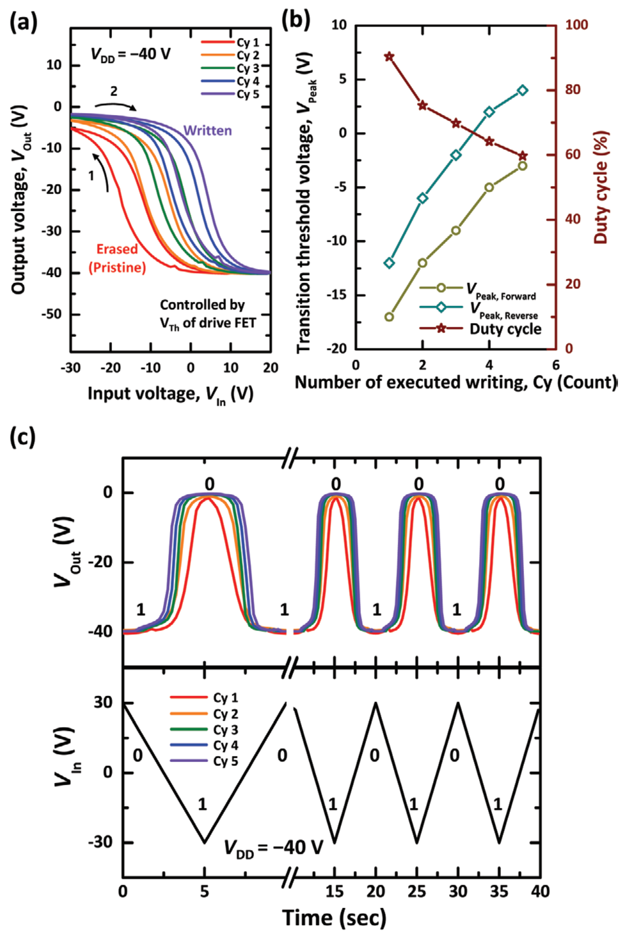

Figure 5. a) Output voltage (V_{Out}) transfer characteristics, b) transition threshold voltage (V_{Peak}) with duty cycle, and c) V_{Out} of an inverting Schmitt trigger at a fixed power supply voltage (V_{DD}) of –40 V in accordance with the repeat writings.

ferroelectric depletion load inverter. As described in Figure 3, the transition threshold voltages of the inverter, that is, the position of the gain peaks, can be freely adjusted by using nonvolatile characteristics of the two-in-one device. From the fully erased state, V_{Out} transfer characteristics at a fixed V_{DD} of –40 V shifted to higher potentials consistent with the repeat writing results, as shown in **Figure 5**a. Accordingly, the transition threshold voltages also shifted to higher potentials and the difference between the two transition threshold voltages broadened as shown in Figure 5b. Here, the execute condition was that V_G and V_D had to be fixed at −30 and −10 V, respectively, for 5 s to drive the transistor. In terms of the V_{Out} behavior of the inverting Schmitt trigger, which had two different transition threshold voltages but the same triangle input signal, the width of the OFF state became longer while the width of the ON state became shorter according to the number of writing cycles. In other words, a duty cycle, which can be defined as the fraction of a period in which the signal is active, changed from 90.4% to 59.7% as shown in Figure 5b. Although clear step signals could not be obtained due to insufficient gains, pulse widths could be modulated by adjusting the position and gap of the gain peaks. This characteristic can be exploited for pulse width modulation (PWM) applications.

Finally, we developed guidelines based on SPICE simulations on how to design organic Schmitt triggers implemented by a depletion load inverter consisting of p-type or n-type channel materials and ferroelectric or charge trapping mechanisms to achieve inverting or non-inverting characteristics (see Section S2, Supporting Information). These guidelines will be help to determine what Schmitt trigger behavior can be obtained using different channel and/or gate dielectric materials.

3. Conclusion

In this paper, we reported a simple all-solid-state organic Schmitt trigger consisting of twin two-in-one organic ferroelectric memory transistors with the same chemical composition and device dimensions but different threshold voltages. Control of the threshold voltage and hysteresis without any chemical treatment were achieved by polarization switching of photocrosslinked P(VDF-TrFE) in the two-in-one devices.

Various input signals were successfully filtered through the Schmitt triggers and almost the same step shape pulse output signals were obtained. Furthermore, inverting and non-inverting Schmitt triggers were successfully demonstrated by changing the electrode placement and polarity of V_D. In addition, we demonstrated that pulse width could be modulated and used in PWM applications by adjusting the position of the gain peak and the gap by polarization switching of the driver. Finally, we provided guidelines on how to design organic Schmitt triggers with p-type or n-type materials and ferroelectric or charge trapping mechanisms to achieve inverting or non-inverting characteristics. The signal conversions demonstrated in this study can be used for noise filters, one-bit analog-to-digital converters, relaxation oscillators, function generators, switching power supplies, and as basic elements of neuromorphic electronic systems.

The device characteristics (durability to repeated stress cycles, retention time, frequency characteristics, driving voltage) still are not sufficient compared to memory devices using inorganic materials already in practical application. More studies are required on materials to improve the performance of the organic electronic devices. However, we believe that lower power consumption of the device could be achieved by changing the device configuration (thin dielectric layer and narrow channel width, respectively).

We strongly believe that our facile all-solid-state organic Schmitt trigger and the associated design guidelines will inspire future development of integrated organic circuits.

4. Experimental Section

P(VDF-TrFE) (Solvay, 70:30 by moles, M_w: 400K) and dehydrated dimethylformamide (DMF, Aldrich) were commercially purchased. The photo-cross linker, bis-FB-N_3, was synthesized as described in our previous reports.[31,32] p-type Si substrates (NAMKANG HI-TECH CO., LTD.) were ultra-sonicated in various solvents (isopropanol and acetone for 10 min) and dried with nitrogen gas. To fabricate a dielectric thin layer, 70 mg of P(VDF-TrFE) solution was dissolved in 1 mL of DMF. Various amounts of bis-FB-N_3 (5, 10, 15, and 20 mg) were then mixed to the prepared solution and were stirred in an inert globe box at 50 °C for 30 min. Then, the solutions were spin-coated on the Si substrate at 1500 rpm for 2 min. Subsequently, a thin films were irradiated with UV light ($\lambda \approx 254$ nm) for 5 min and annealed at 140 °C for 2 h to photo-activate bis-FB-N_3 in the P(VDF-TrFE) matrix.

The device fabrication of a multi-functional organic ferroelectric memory transistor (channel width of 1000 µm and length of 50 µm) was as follows. The pentacene (50 nm, p-type active layer) and gold (≈50 nm, source–drain electrodes) were deposited through shadow masks by thermal evaporation at each film thickness and under base pressure of ≈10^{-6} torr, respectively. Surface profiler (ET200, Kosaka Laboratory Ltd.) was used to estimate the thicknesses of the thin films. The semiconductor parameter analyzers (HP4145B and Keithley 4200SCS) were performed to characterize the electrical properties of a multi-functional organic ferroelectric memory transistor and organic Schmitt trigger in an inert glove box.

To obtain stable electrical characteristics during repeated measurements, the film fabrication and measurement were performed in inert gas condition (nitrogen filled glove box).[33–35]

In terms of reproducibility of device, the key factor was to avoid moisture as much as possible when fabricating a dielectric layer. Thin film should be fabricated in nitrogen filled dry glove box using dehydrate DMF solvent. By following the above instructions, hysteresis behavior of the device could be effectively excluded by increasing the amount of photocrosslinking to P(VDF-TrFE) through bis-FB-N_3. In addition, it allowed excellent reproducibility of the devices.

Supporting Information

Supporting Information is available from the Wiley Online Library or from the author.

Acknowledgements

This work was supported by the National Research Foundation of Korea (NRF-2020R1A2C2010163) and also partially supported by a Korea Institute for Advancement of Technology (KIAT) grant funded by the Korean Government (MOTIE) (P0002007, The Competency Development Program for Industry Specialist). TL thanks the financial support from the National Creative Research Laboratory program (Grant No. 2012026372) through the National Research Foundation of Korea.

Conflict of Interest

The authors declare no conflict of interest.

Keywords

ferroelectric memory transistors, organic transistors, poly(vinylidene fluoride-trifluoroethylene), pulse width modulation, Schmitt triggers

Received: November 13, 2019
Revised: February 23, 2020
Published online: March 20, 2020

[1] C. Di, Y. Liu, G. Yu, D. Zhu, *Acc. Chem. Res.* **2005**, *42*, 1573.
[2] A. Facchetti, M.-H. Yoon, T. J. Marks, *Adv. Mater.* **2005**, *17*, 1705.
[3] S. Hwang, W. Potscavage, Y. S. Yang, I. S. Park, T. Matsushima, C. Adachi, *Phys. Chem. Chem. Phys.* **2016**, *18*, 29199.
[4] S. Hwang, W. J. Potscavage, R. Nakamichi, C. Adachi, *Org. Electron.* **2016**, *31*, 31.
[5] C. Wang, H. Dong, W. Hu, Y. Liu, D. Zhu, *Chem. Rev.* **2012**, *112*, 2208.
[6] S. Reineke, F. Lindner, G. Schwartz, N. Seidler, K. Walzer, B. Lüssem, K. Leo, *Nature* **2009**, *459*, 234.
[7] G. Li, V. Shrotriya, J. Huang, Y. Yao, T. Moriarty, K. Emery, Y. Yang, *Nat. Mater.* **2005**, *4*, 864.
[8] G. Horowitz, *Adv. Mater.* **1998**, *10*, 365.
[9] J. Ouyang, C.-W. Chu, C. R. Szmanda, L. Ma, Y. Yang, *Nat. Mater.* **2004**, *3*, 918.
[10] H. Sirringhaus, *Adv. Mater.* **2005**, *17*, 2411.
[11] A. C. Arias, J. D. MacKenzie, I. McCulloch, J. Rivnay, A. Salleo, *Chem. Rev.* **2010**, *110*, 3.
[12] H. Matsui, Y. Takeda, S. Tokito, *Org. Electron.* **2019**, *75*, 105432.
[13] W. Tang, Y. Huang, L. Han, R. Liu, Y. Su, X. Guo, F. Yan, *J. Mater. Chem. C* **2019**, *7*, 790.
[14] X. Zhang, W. Deng, R. Jia, X. Zhang, J. Jie, *Small* **2019**, *15*, 1900332.
[15] C. Di, F. Zhang, D. Zhu, *Adv. Mater.* **2013**, *25*, 313.
[16] Y. Guo, G. Yu, Y. Liu, *Adv. Mater.* **2010**, *22*, 4427.
[17] C. R. Newman, C. D. Frisbie, D. A. Da Silva Filho, J. L. Brédas, P. C. Ewbank, K. R. Mann, *Chem. Mater.* **2004**, *16*, 4436.
[18] O. H. Schmitt, *J. Sci. Instrum.* **1938**, *15*, 24.
[19] T. E. Mates, M. L. Chabinyc, S. Bubel, M. S. Menyo, J. H. Waite, *Adv. Mater.* **2015**, *27*, 3331.
[20] J. J. Hopfield, *Proc. Natl. Acad. Sci. USA* **1982**, *79*, 2554.
[21] S. Bharitkar, J. M. Mendel, *IEEE Trans. Neural Networks* **2000**, *11*, 879.
[22] S. Hwang, S. Jang, M. Kang, S. Bae, S.-K. Lee, J.-M. Hong, S. H. Lee, G. Wang, S. Fabiano, M. Berggren, T.-W. Kim, *ACS Appl. Mater. Interfaces* **2019**, *11*, 25358.
[23] R. C. G. Naber, C. Tanase, P. W. M. Blom, G. H. Gelinck, A. W. Marsman, F. J. Touwslager, S. Setayesh, D. M. de Leeuw, *Nat. Mater.* **2005**, *4*, 243.
[24] P. Pavan, R. Bez, P. Olivo, E. Zanoni, *Proc. IEEE* **1997**, *85*, 1248.
[25] S. Jang, E. Hwang, J. H. Cho, *Nanoscale* **2014**, *6*, 15286.
[26] P. Heremans, G. H. Gelinck, R. Müller, K.-J. Baeg, D.-Y. Kim, Y.-Y. Noh, *Chem. Mater.* **2011**, *23*, 341.
[27] Y. J. Shin, S. J. Kang, H. J. Jung, Y. J. Park, I. Bae, D. H. Choi, C. Park, *ACS Appl. Mater. Interfaces* **2011**, *3*, 582.
[28] R. C. G. Naber, K. Asadi, P. W. M. Blom, D. M. de Leeuw, B. de Boer, *Adv. Mater.* **2010**, *22*, 933.
[29] B. E. Park, in *Ferroelectric-Gate Field Effect Transistor Memories* (Eds: B. E. Park, H. Ishiwara, M. Okuyama, S. Sakai, S. M. Yoon), Topics in Applied Physics, Vol. *131*. Springer, Dordrecht **2016**, p. 141.

[30] S. W. Jung, S. M. Yoon, S. Y. Kang, B. G. Yu, *Integr. Ferroelectr.* **2008**, *100*, 198.
[31] Y. Ji, D. F. Zeigler, D. S. Lee, H. Choi, A. K. Y. Jen, H. C. Ko, T. W. Kim, *Nat. Commun.* **2013**, *4*, 2707.
[32] S. X. Cai, J. C. Nabity, M. N. Wybourne, J. F. W. Keana, *Chem. Mater.* **1990**, *2*, 631.
[33] L. Feng, W. Tang, J. Zhao, R. Yang, W. Hu, Q. Li, R. Wang, X. Guo, *Sci. Rep.* **2016**, *6*, 20671.
[34] A. Benor, A. Hoppe, V. Wagner, D. Knipp, *Org. Electron.* **2007**, *8*, 749.
[35] A. Vollmer, O. D. Jurchescu, I. Arfaoui, I. Salzmann, T. T. M. Palstra, P. Rudolf, J. Niemax, J. Pflaum, J. P. Rabe, N. Koch, *Eur. Phys. J. E* **2005**, *17*, 339.